16th Australasian Fluid Mechanics Conference
Crown Plaza, Gold Coast, Australia
2-7 December 2007

CFD simulation of wave run-up on a spar cylinder

Nitin Repalle[1], Krish Thiagarajan[1] and Michael Morris-Thomas[2]

[1]School of Mechanical Engineering
University of Western Australia, Western Australia, 6009 AUSTRALIA

[2]Department of Marine Technology,
Norwegian University of Science and Technology, NO-7491, NORWAY

Abstract

A spar is essentially a large cylindrical deep draft floating facility which is promising technology for deep sea platforms because of its excellent sea keeping characteristics and its ability to support either rigid or flexible risers. However one of the most important factors in keeping the spar platform stable is to accurately determine the required air gap (region between the mean water level and the freeboard). A Reynolds Averaged Navier Strokes (RANS) based model is presented to model the wave run-up around the spar cylinder. The model enables one to calculate the maximum wave heights that an offshore platform may face. Results, presented for a typical spar cylinder compare well with the expected results of past empirical methods found in the literature.

Introduction

As the demand for oil and gas increased exponentially over the past 2-3 decades, it lead engineers to move towards designing floating production facilities starting from the conversion of oil tankers into floating production storage and offloading (FPSO) ships to the impressive Tension Leg Platforms but the most innovative deep water floater to be developed was the spar. A classic spar platform consists of a large-diameter, single vertical cylinder supporting a deck.

The ability of the spar to both weather the worst storm conditions and its deep water potential has seen the spar be considered in many of the world's deep offshore reserves. As oil and gas production move to deeper waters, the deck height of the spar is limited by the enormous size of the hull and stability demands, thus accurate prediction of the required air gap above the free surface is given prominence. The wave run-up phenomenon is the vertical up rush of water that is a result of an incident wave train breaking on a partially immersed body.

CFD simulations

Computational Fluid Dynamics is an important tool to recreate phenomena such as wave run-up and thus aids in understanding the underlying factors causing it. As the increasing use of CFD in engineering analysis is evident it is important to make sure that the results from the simulation are in tandem with the theoretical and published results. Wave run-up for a single cylinder column is a problem of interest over the past 6 decades McCamy and Fuchs [1] solved this problem analytically by extending Havelock's linear potential theory. We find Kriebel [2], Niedzwecki and Hustron [3], treating the problem using the second order solutions.

The CFD calculations shown here are based on simulated solutions to the Reynolds Averaged Navier-Stokes (RANS) equations, carried out using FLUENT software. The prediction of the free surface in the package is based on the volume tracking method VOF (Volume Of Fluid). This method is developed to simulate highly nonlinear effects such as breaking waves at the interface, although, no such breaking effects have been observed in the current analysis. For wave propagation problems, special boundary treatments have been devised in Fluent. The outflow boundary condition is set in such a way as to allow their continuation through the boundary with a minimum of reflection.

A numerical wave tank has been modelled, whose geometry was chosen to simulate the experimental conditions of Paterson (2004)[4]. Figure 1 gives the representation of the model test tank.

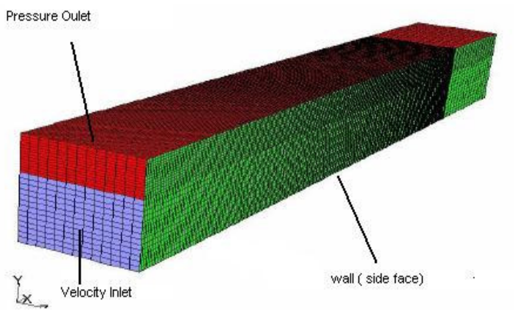

Figure 1: Test tank domain with boundaries applied.

Waves are generated at the left boundary (inlet) and propagate to the right. A user defined function (UDF) reproduces the Stokes second order waves. The waves are gravity driven. The appropriate equations defined in the UDF are given by the following equations

X – velocity

$$u = Agk\frac{\cosh k(h+z)}{\omega \cosh kh}\cos(kx-\omega t) + A^2\omega k\frac{\cosh 2k(h+z)}{\sinh^4(kh)}\cos 2(kx-\omega t) \quad (1)$$

Y – velocity

$$w = Agk\frac{\sinh k(h+z)}{\omega \sinh kh}\sin(kx-\omega t) + A^2\omega k\frac{\sinh 2k(h+z)}{\cosh^4(kh)}\sin 2(kx-\omega t) \quad (2)$$

Here A, k and w are the wave amplitude, wave number and wave angular frequency respectively. The resultant second order wave elevation profile is given by

$$\eta = A\cos(kx - \omega t) + \frac{A^2 k \cosh(kh)}{4\sinh^3(kh)}[2 + \cosh(2kh)]\cos 2(kx - wt) \qquad (3)$$

The still water depth (h) is 1.2 m (Z direction) while the total height of the domain is 2 meters. The width is 2 m (Y direction) and the length is 15 m (X direction). The cylinder used here is 0.8m high with 0.2m diameter. The draft of the cylinder remains at 0.4 metres while the position of the cylinder from the front face is approximately 3.5 metres from the centre of the cylinder and at a distance of 1m from the side walls as shown in Figure 2.

The VoF method requires discretization of the full domain including the volume above the free surface. Broadly the domain is discretized in to cells of length of 0.01m except for the near cylinder region. An unstructured hexahedral mesh with 204295 elements is used to mesh the domain. The mesh size along the final 5 meters length progressively becomes larger at a ratio of 1.05. The meshing scheme used to model is mapped mesh as this provides for a more structured mesh with tetrahedral elements.

The solver solution controls utilised in the run-up simulations are the body force weighted pressure discretisation with the PISO pressure velocity coupling. The momentum transport equation discretisation was used with the MUSCL third order and the modified high resolution interface capturing (HRIC) options. Both the MUSCL third order an HRIC provide the RANS solver with increased solution power for breaking waves and other complex multiphase problems. The default values were kept for all the other settings. SIMPLE algorithm was chosen to recreate the pressure velocity coupling and the second order upwind method was used for the momentum transport equations and for the free surface tracking. A rake of surface probes are used to capture the information from the wave. Three probes were positioned at a distance of 2 m, 3.9 m and 10 m from the left boundary to measure incident wave and formation of any reflected waves. A sample of wave profile around the cylinder is shown in Figure 3.

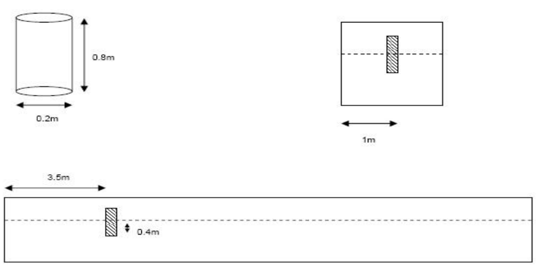

Figure 2 : Location and geometry of the cylinder

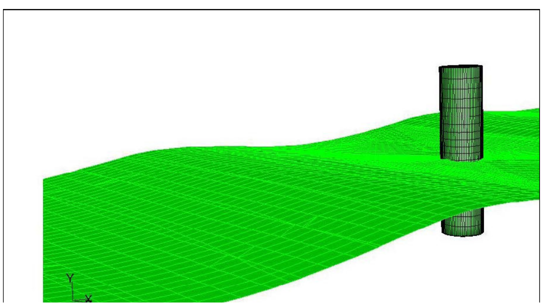

Results

Verification of Test tank

The UDF was given input of period T = 1.13s, wave height H=0.2m and wave length L = 2m. The velocities as measured on probe at positions 2, 4 and 6 metres along the x-axis of the tank. The figure show the Stokes second order velocities for time t=10 s. Figure 4 clearly shows a good comparison between the FLUENT simulation and the theoretical Stokes second order solution at x = 4 m. This verification thus indicates that the test tank and underlying mesh scheme will be suitable for the coming cylinder simulations. The profiles at x = 2 and 6m are offset from the theoretical line, and could be the result of the 1.2 metre water depth being too shallow and thus causing the wave to behave like a long wave, thus having an effect on the wave length and period.

Run-Up results

A comparison with the linear diffraction theory [1] for the run up ratio (wave run up at the face of the cylinder/ wave amplitude) is presented in Figure 5. Here $ka = 2\pi a/L$ is the scattering parameter depending upon the wavelength L and cylinder radius a. Also shown are the experimental data from Paterson [4]. The linear theory produces a lower bound for the wave run-up. This has been documented in other research papers surrounding run-up since the introduction of the solution by Havelock. This includes Isaacson [5] who suggested that the linear solution should be scaled up by a factor of 40%, Kriebel[6] who found that the linear diffraction error was as much as 85% in some cases and Morris-Thomas & Thiagarajan[7] whose results found that the linear diffraction theory severely under predicted the run up ratio.

When a comparison is made between the two smallest values of ka the influence of the non linearities can be seen clearly. At these values of wave scatter the FLUENT results predict

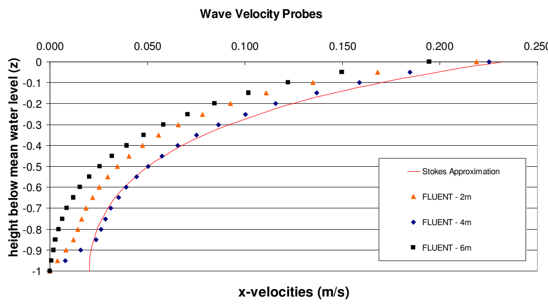

Figure 4: Measured results of the velocities under the wave compared to the theoretical Stokes second order solution

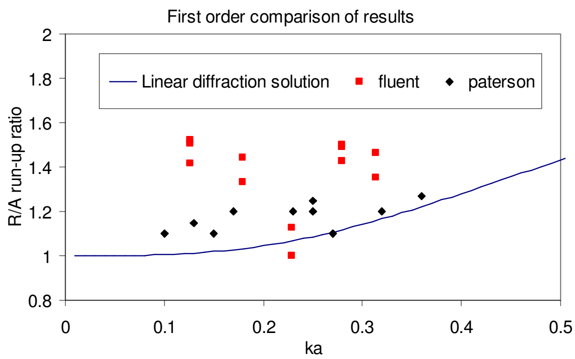

run-up ratios that approximate the ratios predicted at wave scatter parameters of twice these values. The effect of the *kA* values, represented by the vertical spacing of the results conforms to the conclusions of Morris-Thomas and Thiagarajan [7] that the run-up ratio is highly dependent upon both wave scatter and wave steepness.

We next show comparison of FLUENT results for wave run up at the face of the cylinder vs. the incident wave profile. Figures 6 and 7 show these profiles for two different *ka – kA* parameter combinations. The extent of the run-up can be clearly seen on the figures. The incident wave builds up first as this position is closest to the velocity inlet whilst the run-up takes more time to build up as it is further from the boundary

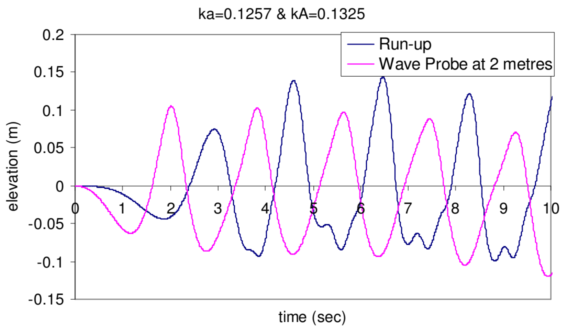

Figure 6: Wave profiles for incident wave and run-up for ka=0.2793 and kA=0.2793

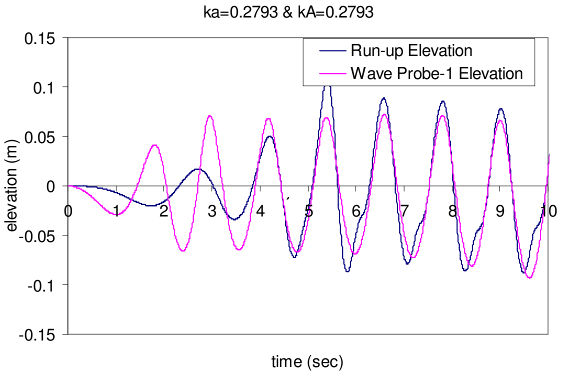

Figure 7: Wave profiles of incident wave and run-up for ka=0.1257 and kA=0.1325

and the effects of the wave-structure interaction have not yet built up fully. Thus we see that the run-up profile takes two to three wave lengths to build up. A further observation is that the figures display an increasing drop off in the run-up profile and incident wave profile; this observation being more pronounced in figure 7 which has a longer wave length when compared to the other simulations.

Formation of secondary crest

Both Figures 6 and 7 exhibit a secondary crest appearing at the trough of the wave run up profile. This is a consequence of incident wave fronts travelling around both sides of the cylinder and interacting downstream of the structure. The resultant free wave travels upstream and interacts with the oncoming waves causing changes to the wave run up. This phenomenon was also observed experimentally by Morris-Thomas[8].

Figure 8 shows snapshots of free surface elevation at various points of the wave cycle. The correspondence to the wave run up profile is also shown. It can be seen that the crest evolves from the rear of the cylinder once a wave has passed over and interacted with the cylinder. As the wave progresses this crest moves towards the front face of the cylinder and interacts with the new incident wave forming the secondary crest. At some point the amplification of the crest dissipates and together with this the run-up profile returns to normal. One important observation from the simulation tests is that the crest is seen in regions of longer wavelength whereas at higher values of wave number and low wave amplitudes the secondary crest does not seem to occur. Further, the interaction of the crest with the oncoming waves depends strongly on the phase difference between them, which in turn depends on the wavelength and cylinder circumference. Careful observation of Figures 6 and 7 shows the movement of the secondary crest relative to the "original" trough location of the wave run up. This has important consequence on the maximum run up estimation as will be shown presently.

Run-up ratio comparison

The third order solution presented here is based upon the long wave length theory, which defines the free surface elevation as follows

$$\zeta = \zeta_1 + \zeta_2 + \zeta_3 + O(\varepsilon^4) \qquad (4)$$

Where ζ_1 , ζ_2 and ζ_3 are the first, second and third order free surface elevations computed at the cylinder surface. This is a closed form solution to the wave run up problem under the

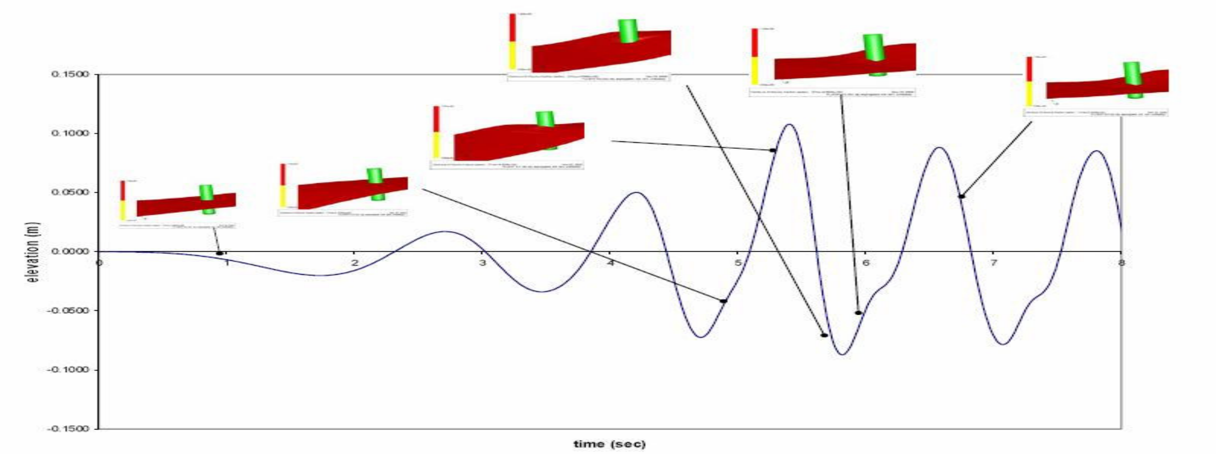

assumption of long wavelength. More details may be found in Morris-Thomas [8]. Although the input waves are of second order, the third order LWL solution is used as a proxy for the second order diffraction solution. Figure 9 shows maximum wave run up (estimated as half of the max peak-to-trough value) to wave amplitude ratio vs. steepness (*kA*) for three different scattering parameter (*ka*) values.

Wave scatter parameter = 0.2793 and above

The run up value is seen to be about 50% more than the incident wave amplitude. Here the LWL theory predicts the maximum run up ratio quite well. In this region the non linear secondary crest is dominant whilst the LWL theory is applicable. The simulated run up seems to decrease with increasing kA, and this is not the trend seen in the theory. More data will be needed to substantiate this difference.

Wave Scatter parameter = 0.2285

This region shows a marked decrease in wave run up, even lower than theoretical prediction. From Figures 6 and 7, it is seen that there is an intermediate ka value similar to 0.228 where the secondary crest is 180 deg out of phase and has a maximum cancellation effect of the incident wave run up. Again a decreasing trend with kA is observed here.

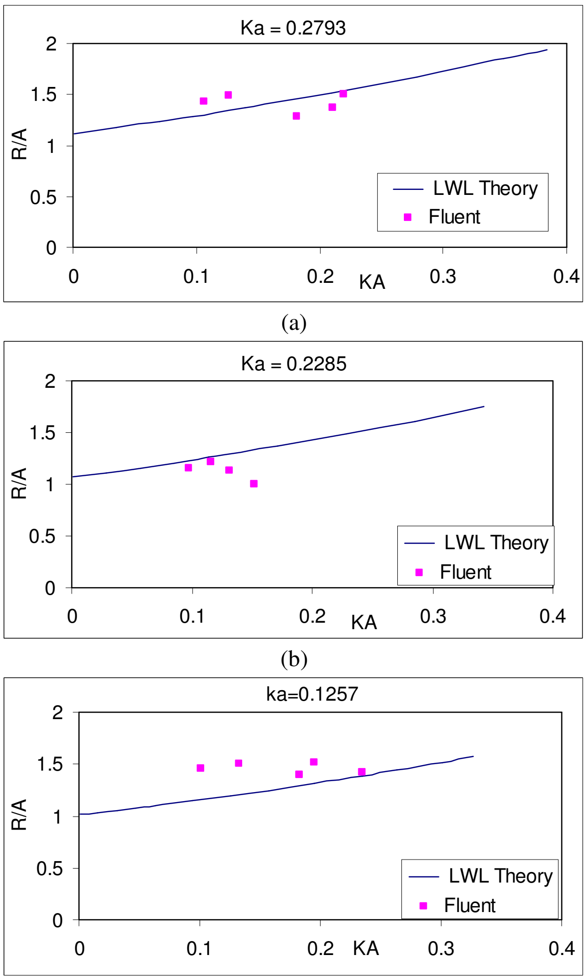

(a)

(b)

(c)

Figure 9: Maximum run up to wave amplitude vs. *kA*; comparison between Fluent and LWL theory.

Wave Scatter = 0.1275 and below

In this region the under prediction of theory for $kA < 0.16$ is most probably due to this region being more applicable to a Stokes second order expansion. In the region $kA > 0.16$ the non-linear crest appears and thus together with this the third order theory over predicts the simulation. Here a superposition effect may be causing the amplification to the free surface subsequently altering the run-up ratio.

Conclusion

The CFD code implemented through industry software FLUENT is validated against the theoretical / published results. It has been shown that the code replicates severe nonlinearities in the wave run-up that occur at low values of ka which are not accounted in second order diffraction theory or the third order long wave length theory. Comparison of free surface profile confirms that CFD code can reproduce acceptable profile around the cylinder though there are some discrepancies between the measured and computed values. Refinement of mesh around the cylinder wall and repeating the simulations on powerful processing unit is required for a more substantial picture of the run-up and associated nonlinearities.

Acknowledgements

The authors acknowledge the financial support of the UWA Grants Scheme. Fluent academic licence is distributed by LEAP Australia. Earlier versions of the UDF's were developed and tested by M Horko, Y Li, and A. Arima.

References

[1] McCamy, R. and Fuchs, R. (1954), "Wave Forces on Piles: A Diffraction Theory", *Tech. Memo No. 69,, U.S. Army Corps of Engrs,* Washington D.C, USA.

[2] Kriebel, D. L. 1990. Nonlinear wave diffraction by vertical circular cylinder. Part 1: Diffraction theory. *Ocean Engng,* **17:** 345-377

[3] Niedzwecki, J. M. & Huston, J. R. 1992. Wave interactions with tension leg platforms. *Ocean Engng*, **19** (1): 21-37

[4] Paterson, F. 2004. An investigation into the efficacy of reduction in wave run-up on vertical cylinders in monochromatic waves by application of dampening fins. Honours' thesis, The University of Western Australia

[5] Isaacson, M. de St. Q. 1978. Wave run-up around large circular cylinder. *J Waterway, Port, Coastal and Ocean Eng, ASCE*, **104** (4): 69-79

[6] Kriebel, D. L. 1992. Nonlinear wave interaction with a vertical circular cylinder. Part 2: Wave runup. *Ocean Engng,* **19** (1)**:** 75-99

[7] Morris-Thomas, M. T. and Thiagarajan K. P. (2004). The run-up on a cylinder in progressive surface gravity waves: harmonic components. *Appl. Ocean Res.* **26**: 98-113

[8] Morris-Thomas, M. T., (2003) Wave run up on vertical columns of an offshore structure, PhD Thesis, The University of Western Australia.